Computation of oscillator strengths from Kohn–Sham wave functions: the example of small lithium clusters

Georges Gardet, François Rogemond, Henry Chermette
Institut de Physique Nucléaire de Lyon, IN2P3-CNRS et Université Claude Bernard,
43, Bd du 11 Novembre 1918, F-69622 Villeurbanne Cédex, France

Summary. Density functional calculations of ground and excited states of Li_n ($n \leqslant 8$) clusters have been performed, within two different approaches. Using a set of Kohn–Sham orbitals to construct wave functions, the calculation of the oscillator strengths of the electric dipole transitions is performed. Our results have been tested at two levels: first the necessary comparison with the experimental data, second the comparison with high level CI (MRD-CI) calculations. This last point is not a trivial challenge, because such an *ab initio* method leads for small clusters to a highly accurate description of the electronic structure and optical absorption spectra. Finally, this is also a new test for the capability of using Kohn–Sham orbitals to construct physically meaningful wave functions.

Transition energies, oscillator strengths and finally optical absorption spectra presented here are in general in reasonable agreement with the experimental data and the MRD-CI calculations. That is very promising for bigger systems, with regard to the modest computational effort (CPU time and memory size) of density functional calculations.

1 Introduction

Theoretical investigations of the electronic features of the ground state (GS) and the excited states of molecules or clusters play a key role for the interpretation of the experimental data such as ionization potentials or optical spectra. For example, structural information about small alkali metal clusters (Li_n, $n \leqslant 8$) have recently been carried out, in part from the comparison between *ab initio* calculations with post-Hartree–Fock configuration interaction (CI) and optical absorption spectra [1–4]. However, it is well known that such high level CI or Moller–Plesset calculations are quite expensive in computational resources, since they scale (at least) as n^5, n being the number of electrons. This precludes the use of such a method for significantly larger systems.

On the other hand, density functional theory (DFT) has proved to be able to provide valuable results about structural and energetic properties of molecules,

clusters, or molecules adsorbed on surfaces using a set of Kohn–Sham (KS) orbitals (for an extensive review of the capabilities of the method, see Ziegler [5]). Recently, several works [6] have proved that Slater determinants of KS orbitals are physically meaningful wave functions of the ground state of a system with a given electron density. Using the extension of the Hohenberg and Kohn theorem [7] to excited states (see further), the wave functions of some excited states are obtained similarly. From this starting point, the electric dipole transition moments can be computed and, finally, the oscillator strengths of the transitions and the theoretical absorption spectra are estimated.

In this paper, the accuracy and predicting power of DFT to obtain oscillator strengths and to model absorption spectra are investigated. First the calculations of the transition energies and the computation of the transition moments are called. Then, applications to the absorption spectra of some Li_n clusters ($n \leqslant 8$) are given. Li_n clusters are good candidates to test DFT because for such systems both recent theoretical and experimental results are available and, moreover, computing time is reasonable.

Our structural or energetic results have been carried out using the ADF [8] or the deMon [9] code, with local or gradient-corrected potentials. The transition moments proceed from a special routine added to the deMon code.

2 Transition energies

2.1 Multiplet approach

The Hohenberg and Kohn theorem assumes that all the properties of the GS of a physical system (in particular its energy) can be determinated from its electron density. The Gunnarson–Lunqvist extension to excited states [10] provides a way to obtain the excitation energies. This way has been earlier developed by Ziegler et al. [11] and Von Barth [12] and their calculations afford results in reasonable agreement with experiments. More recently it has been extended to any irreducible representation by Daul [13]. Thus it is possible to describe the multiplet splitting at least to first order. In particular, Daul et al. [14] have recently given some results for the ruthenocene molecule in excellent agreement with the properties derived from the optical spectroscopy. This method based on vector coupling gives for any symmetry point group the relation between the multiplet splitting and the single-determinant energies of a molecule or cluster, including the case of degenerate orbitals. The corresponding computer programs have been also developed by Daul. Following this technique, the multiplet wave function:

$$\Psi_i = |\alpha \Gamma m_\Gamma S m_S\rangle,$$

arising from a given configuration α, is obtained by vector coupling as a linear combination of single determinants:

$$\Psi_i = \sum_\mu A_{i\mu} \Phi_\mu, \qquad (1)$$

where Γ is the label of the irreducible representation of the space part of the wave function; m_Γ refers to its component in case of degeneracy; S is the spin part of the wave function with component m_S in case of spin multiplicity larger than 1, Φ_μ is a single Slater determinant and $A_{i\mu}$ is a matrix of symmetry coefficients which is

given by a first program. Then, the second and third programs give the single determinant energies $E(\Phi_\mu)$ in terms of the r non-redundant single determinants Φ_j:

$$E(\Phi_\mu) = \sum_{j=1}^{j=r} C_{\mu j} E(\Phi_j)$$

and finally the multiplet energies:

$$E(\Psi_i) = \sum_{j=1}^{j=r} F_{ij} E(\Phi_j). \tag{2}$$

It should be noticed that Eq. (2) gives the energy to first order, since only Coulomb and exchange integrals (first-order electrostatic interaction) contribute to the single-determinant Φ_j.

2.2 Fritsche approach

From a totally different point of view, Fritsche [15] developed recently the generalized DFT, which affords for the solids the energies of any eigenstate of N interacting electrons from the density of the GS only. Assuming that the extension to clusters is legitimate, the excitation energy would be given by

$$\Delta E = \varepsilon_f - \varepsilon_i + \Delta_{fi}, \tag{3}$$

with

$$\Delta_{fi} = -\int \Delta \rho^0_{fi}(r) [V^i_{xc}(r) - 2\varepsilon^i_{xc}(r) \, dr$$

and

$$\Delta \rho^0_{fi}(r) = |\phi_f(r)|^2 - |\phi_i(r)|^2,$$

where ε is a KS eigenvalue, the subscripts i and f refer to the two KS orbitals ϕ involved in the one electron transition, the superscript i refers to the ground state, $\varepsilon^i_{xc}(r)$ and $V^i_{xc}(r)$ are, respectively, the exchange-correlation energy per particle and the exchange-correlation potential. Note that Eq. (3) is obtained assuming that the excited state is a single determinant.[1]

---

[1] On the basis of different hypotheses, Malkin et al. [26] proposed recently a similar, but different, form for the transition energy, namely:

$$\Delta E = \varepsilon_f - \varepsilon_i + \Delta_{fi},$$

with

$$\Delta_{fi} = -\int \frac{\rho_f(r)\rho_i(r)}{\rho^\uparrow} [V^i_{xc}(r) - \varepsilon^i_{xc}(r)] \, dr$$

and

$$\rho_f(r) = |\phi_f(r)|^2,$$

$$\rho^\uparrow = \sum_j |\phi^\uparrow_j(r)|^2.$$

2.3 Calculations

To perform our calculations, the geometries of the Li_n clusters have been first optimized at the local density approximation level (LSD) and, for Li_3 and Li_4, further optimized at the non-local (i.e. gradient-corrected) level of approximation (in this last case we used the correlation functional of Perdew [16] and the exchange functional of Becke [17]). The equilibrium geometries are found very close to those found by post-Hartree–Fock calculations [1–4]. They are labelled with the symmetry group symbols. The details on the structure calculations will be published elsewhere [18].

Our results have been obtained within the two approaches in the energy range from 1 to 4 eV. For the multiplet calculations, we have taken into account all the configurations corresponding to singlet and triplet LSD states for the even values of n, and to doublet and quadruplet LSD states for the odd ones.

3 Oscillator strengths

3.1 Method

For an atomic system, assuming an L–S coupling and neglecting the spin–orbit interaction, the length form of the multiplet oscillator strength f is given by the expression [19]:

$$f = \frac{2}{3} \frac{E' - E}{(2S + 1)(2L + 1)} \sum_{M_L = -L}^{+L} \sum_{M_S = -S}^{+S} \sum_{M_{L'} = -L'}^{+L'} \sum_{M_{S'} = -S'}^{+S'} |\langle \Psi | R | \Psi' \rangle|^2,$$

where $|\Psi\rangle$ and $|\Psi'\rangle$ are the normalized initial and final states involved in the electric dipole transition with the energies E and E' (resp.),

L and L' are the angular moments (resp.), S and S' the spins (resp.), $(2S + 1)(2L + 1)$ is the degeneracy of the initial state, R is the position operator:

$$R = \sum_{i=1}^{n} r_i,$$

n being the number of electrons.

A similar expression can be written for molecules or aggregates:

$$f = \frac{2}{3} \frac{E' - E}{(2S + 1)(m_\Gamma)_{max}} \sum_{m_\Gamma = 0}^{(m_\Gamma)_{max}} \sum_{M_S = -S}^{+S} \sum_{m_{\Gamma'} = 0}^{(m_{\Gamma'})_{max}} \sum_{M_{S'} = -S'}^{+S'} |\langle \Psi | R | \Psi' \rangle|^2,$$

where $|\Psi\rangle = |\alpha \Gamma m_\Gamma S m_S\rangle$ and $|\Psi'\rangle = |\alpha' \Gamma' m_{\Gamma'} S' m_{S'}\rangle$ are the initial and final states. In the present work, $|\Psi\rangle$ refers to the ground state of the system and $|\Psi'\rangle$ to a one-electron excitation (a doubly or more excited configuration, which is generally associated with small oscillator strengths describes fine effects and is beyond the scope of this work).

Following the procedure of Daul, the transition moment

$$M = \langle \Psi | R | \Psi' \rangle$$

can be written as

$$M = \sum_{\mu\nu} A_\mu A'_\nu \langle \Phi_\mu | R | \Phi'_\nu \rangle,$$

where $\langle \Phi_\mu | R | \Phi_\nu' \rangle$ are matrix elements of the R operator between the two determinants Φ_μ and Φ_ν' which are, respectively, connected to the ground state and the excited state by Eq. (1). Thus, to obtain M it is necessary to compute all the $\langle \Phi | R | \Phi' \rangle$ (the index of the Slater determinants has been omitted because there is no more ambiguity) where

$$\Phi = (n!)^{-1/2} \sum_j (-1)^j P_j(\phi_{j_1}(1)\phi_{j_2}(2) \dots \phi_{j_n}(n))$$

and

$$\Phi' = (n!)^{-1/2} \sum_k (-1)^k P_k(\phi_{k_1}'(1)\phi_{k_2}'(2) \dots \phi_{k_n}'(n)),$$

$\{\phi_i\}_{i=1,n}$ and $\{\phi_l'\}_{l=1,n}$ are the Kohn–Sham spin orbitals, building blocks of Ψ and Ψ' respectively.

In the expression of Φ (or Φ'), the jth (or kth) term of the sum is simply obtained by applying the permutation operator P_j (or P_k) to the KS spin orbitals and multiplying by -1 or $+1$, according to the parity of the P_j (or P_k) operator.

Let us recall here that Eq. (3) has been derived by Fritsche assuming that the excited state χ is described by a single determinant X. Following this approach, the oscillator strength of the transition $\Phi \to \chi$ is simply given by

$$f_F = \tfrac{2}{3} \Delta E |M_F|^2$$

where the transition moment is

$$M_F = \langle \Phi | R | X \rangle$$

(Φ being a GS determinant) which is mathematically analogous to $\langle \Phi | R | \Phi' \rangle$ and will be computed similarly.

Introducing the expressions for Φ and Φ', $\langle \Phi | R | \Phi' \rangle$ can be expressed as

$$\langle \Phi | R | \Phi' \rangle = \frac{1}{n!} \sum_j (-1)^j P_j \sum_k (-1)^k P_k \langle \phi_{j_1}(1) \dots \phi_{j_n}(n) | \sum_{i=1}^n r_i(i) | \phi_{k_1}'(1) \dots \phi_{k_n}'(n) \rangle$$

It is well known that such an expression can be dramatically simplified [20]:

$$\langle \Phi | R | \Phi' \rangle = \sum_{i=1}^n \sum_r (-1)^r P_r \langle \phi_{r_1}(1) \dots \phi_{r_n}(n) | r_i(i) | \phi_1'(1) \dots \phi_n'(n) \rangle, \qquad (4)$$

where P_r runs only over the $n!$ permutations in the $\{\phi_i\}_{i=1,n}$ (and no more in the $\{\phi_i'\}_{l=1,n}$).

Moreover, since $r_i(i)$ is a one-electron operator, all the terms of the sum in (4) break up into a product:

$$P_r \langle \phi_{r_1}(1)\phi_{r_2}(2) \dots \phi_{r_n}(n) | r_i(i) | (\phi_1'(1)\phi_2'(2) \dots \phi_n'(n) \rangle$$

$$= \langle \phi_{r_1}(1) | \phi_1'(1) \rangle \cdots \langle \phi_{r_i}(i) | r_i(i) | \phi_i'(i) \rangle \cdots \langle \phi_{r_n}(n) | \phi_n'(n) \rangle. \qquad (5)$$

It should be noticed that $\langle \phi_{r_p}(p) | \phi_p'(p) \rangle$ and $\langle \phi_{r_s}(q) | r(q) | \phi_q'(q) \rangle$ do not depend on the p or q index of the electrons, and that in general

$$\langle \phi_j | \phi_l' \rangle \neq \delta_{jl}.$$

The rigorous calculation of M needs the computation of the $n!$ permutations P_r of the $\{\phi_i\}_{i=1,n}$ in Eq. (4) and our algorithm takes into account all these

permutations, but of course, all these terms are not computed usque ad finem: in fact, $\langle \phi_{r_i} | r | \phi_i' \rangle$ excepted, all the factors of the right-hand side in Eq. (5) are smaller or equal to unity. Using the Schwartz inequality, it can be shown easily:

$$| \langle \phi_j | \phi_i' \rangle |^2 \leqslant \langle \phi_j | \phi_j \rangle \langle \phi_i' | \phi_i' \rangle,$$

where $\langle \phi_j | \phi_j \rangle$ and $\langle \phi_i' | \phi_i' \rangle$ are equal to unity. (Moreover, although $\langle \phi_j | \phi_i' \rangle$ is not equal to δ_{jl}, its numerical value is in practice, in most cases, very close to zero or unity, except for a small number of factors.) Thus, as soon as the product of $\langle \phi_{r_i} | r | \phi_i' \rangle$ by the p first factors $\langle \phi_{r_n} | \phi_n' \rangle$ in Eq. (5) becomes smaller than a given criterion (typically from 10^{-4} to 10^{-6}), the program stops and the corresponding term in Eq. (4) is dropped. The numerical stability of M for several criteria with different orders of magnitude assumes that the dropped terms in Eq. (4) are negligible (Table 1 shows the example of the 1.73 eV-B_2 transition in $Li_6(C_{2v})$).

3.2 Normalized oscillator strengths

As can be seen from the definition, the oscillator strength consists of two important factors: the transition energy ΔE and the transition moment M. Of course, an inaccurate value of ΔE induces an error in the oscillator strength. Then, to permit an objective estimation of the quality of oscillator strengths with the "multiplet approach", the transition energies are taken from our "multiplet" calculations, except in the case of disagreement with the experimental values. In these last cases, the energy values derived from the Fritsche method have been used. Obviously, this is only a way to compare our DFT oscillator strengths with those of the MRD-CI calculations. Such a "correction" cannot be made *a priori* without experimental or other computed data and each spectrum given in the last part of the section proceeds from only one approach.

It is well known that the oscillator strengths are very sensitive to the quality of the wave functions of the states involved in the transition [21]. Recently, *ab initio* calculations of Bauschlicher et al. [22] showed that basis sets, correlation treatment, geometrical parameters, length or velocity form, can induce important variations of the oscillator strength, without any change of the total energy (It should be noticed that in this last paper [22], the length form is shown as the more stable). More precisely, Fuchs et al. [23], in their work on Na_6 show that direct comparison between the oscillator strengths derived from different approximations are not relevant. For example, in their large-scale multiconfigurational

Table 1. Transition moment calculations for 1.73 eV-B_2 transition of $Li6(C_{2v})$

Criterion	Transition moment
10^{-1}	1.7
10^{-2}	1.92
10^{-3}	1.971
10^{-4}	1.9825
10^{-5}	1.98444
10^{-6}	1.984762
10^{-7}	1.9848000
10^{-8}	1.98480052

linear response calculations, the absolute values of the oscillator strengths depend strongly on the size of the active space: great variations of the oscillator strength corresponds to a transition of a given irreducible representation may be counter balanced by another one in the same energy range, so that the theoretical spectrum does not show any significant change and is even in satisfactory agreement with the experimental spectrum. Therefore it is not surprising to obtain DFT absolute oscillator strengths which are larger than MRD-CI values. This may be related to factors like basis sets as well as the selected theoretical method, or the equilibrium geometry. Accordingly in Tables 4–7 we have used "normalized oscillator strengths"

$$\tilde{f}_n = \frac{f_n}{\sum f_n},$$

with eventually the global value for a narrow energy range in case of quasi-degeneracy.

4 Results and discussion

4.1 Transition energies

The excitation energies obtained for the rhombus $Li_4(D_{2h})$, the tripyramid $Li_6(C_{2v})$, the tetracapped tetrahedron $Li_8(T_d)$ clusters within the two different approaches are gathered in Table 2 for the largest intensity transitions (resonance) with MRD-CI oscillator strengths in the range of 1, and in Table 3 for those with oscillator strengths in the range of 0.1. For the sake of complete comparison, the experimental and MRD-CI data have been reported. In this Table 3 have been added two transition energies for the triangle $Li_3(C_{2v})$ and one value from a coupled electron pair approximation calculation [24]. To our knowledge, surprisingly, no other *ab initio* oscillator strengths are available. Therefore, for this cluster, only a comparison between experimental [25, 1, 4] and computed absorption spectra will be reliable. For the clusters larger than Li_4 the geometries used were those optimised at the LSD level whereas the non-local level was retained for Li_3 and Li_4, as stated previously.

One can see in Tables 2 and 3 that the energetic positions of the multiplets are in agreement with the experimental or CI values, except for the first intense transition in Li_4 (D_{2h}) and Li_6 (C_{3v}). These transitions involve for Li_4 (D_{2h}) [1] some states for which the description of the electron correlation requires, in the CI method, at least two determinants of different configurations with coefficients of the same order of magnitude. The DFT computes several determinants related to only one configuration and leads in this case to a crude description. For such a transition a more sophisticated gradient-corrected functional is needed. In the case of $Li_6(C_{3v})$, as pointed out by Daul, the discrepancy may be related to the formula (2), which is only a first-order expression for the energy. It would be interesting to compute the off-diagonal terms (second-order electrostatic contributions) to check the effect of this approximation on this transition.

It is worthwhile to note that the Fritsche scheme works well with the transitions of large intensity. We can see in Table 2 (large intensity transitions) that in all cases the transition energy computed within the Fritsche scheme looks in reasonable agreement with the CI values: the rms deviation is about 8%. However, this

Table 2. Comparison of DFT transition energies (in eV) with "multiplets" or Fritsche approach, MRD-CI values (Ref. [1,2]), and experimental results (Ref. [1–4]). This table has been limited to the main transitions, with oscillator strength in MRD-CI calculations in the range of 1

Cluster	Experimental position	DFT symmetry state	DFT-multiplet transition energy	DFT-Fritsche transition energy	MRD-CI symmetry state	MRD-CI transition energy	MRD-CI oscillator strength
Li_4 (D_{2h})	1.801	B_{3u}	1.42	1.92	$1B_{3u}$	1.78	0.7926
Li_4 (D_{2h})	2.651	B_{2u}	2.35	2.38	$1B_{2u}$	2.65	0.6814
Li_4 (D_{2h})	2.928	B_{1u}	3.08	3.30	$1B_{1u}$	3.01	0.5698
Li_6 (C_{2v})	2.2–2.6	B_2	2.27	2.36	$5B_2$	2.40	0.600
Li_6 (C_{2v})	2.2–2.6	A_1	2.41	2.64	$8A_1$	2.51	0.875
Li_6 (C_{3v})		E	1.26	1.90	$3B_2$	2.15	0.91
Li_6 (C_{3v})		A_1	2.13	2.11	$4A_1$	2.19	0.92
Li_8 (T_d)	2.4–2.6	T_2	2.20		$4T_2$	2.41	1.940
Li_8 (T_d)	2.4–2.6	T_2	2.45		$6T_2$	2.63	1.800

Table 3. Comparison of DFT transition energies (in eV) with "multiplets" or Fritsche approach, MRD-CI values (Ref. [1,2]), and experimental results (Ref. [1–4]). This table has been limited to transitions with oscillator strength in MRD-CI calculations in the range of 0.1

Cluster	Experimental position	DFT symmetry state	DFT-multiplet transition energy	DFT-Fritsche transition energy	CEPA transition energy	MRD-CI symmetry state	MRD-CI transition energy	MRD-CI oscillator strength
Li_3 (C_{2v})	c.a. 1.8 [25]		1.68	2.11	1.695 [24]			
Li_3 (C_{2v})	c.a. 2.7		2.60	3.20				
Li_6 (C_{2v})		A_1	1.52	2.13		$2A_1$	1.42	0.100
Li_6 (C_{2v})	c.a. 1.8	B_2	1.73	2.45		$2B_2$	1.73	0.159
Li_6 (C_{2v})	c.a. 1.8	B_2	1.77	2.45		$3B_2$	1.79	0.200
Li_6 (C_{3v})		E	1.55	2.11		$1B_2-2A_1$	1.54, 1.59	0.11 + 0.17
Li_6 (C_{3v})		E	2.80	3.41		$4B_1-10A_1$	2.81, 2.88	0.05 + 0.07
Li_6 (C_{3v})		A_1	2.96	3.41		A_1	3.04	0.20
Li_8 (T_d)		T_2	1.98			$1T_2$	1.45	0.367

G. Gardet et al.

Table 4. Comparison of normalized oscillator strengths $\tilde{f}$ (with $\tilde{f} > 0.005$) for the D_{2h} planar structure of Li_4, computed with "DFT-multiplets" and MRD-CI (from Ref. [1]). The corresponding transition energies (eV) obtained with "DFT-multiplets" or "DFT-Fritsche" (identified by (∗)) and MRD-CI are also reported (see text). All states are labelled within the D_{2h} group

DFT transition energy	DFT symmetry state	DFT oscillator strength	Normalized DFT oscil. strength	Summation due to degeneracy	MRD-CI transition energy	MRD-CI symmetry state	MRD-CI oscillator strength	Normalized MRD-CI oscil. strength
1.92 (∗)	B_{3u}	1.497	0.382	0.382	1.78	$1B_{3u}$	0.7926	0.370
					1.81	$1B_{2u}$	0.0189	0.009
					2.09	$2B_{3u}$	0.0619	0.029
					2.36	$1B_{1u}$	0.0813	0.038
2.04	B_{2u}	0.554	0.141					
2.35	B_{2u}	0.648	0.166	0.307	2.65	$2B_{2u}$	0.6814	0.318
2.86	B_{1u}	0.604	0.154					
3.08	B_{1u}	0.612	0.156	0.310	3.01	$2B_{1u}$	0.5698	0.266

Table 5. Comparison of normalized oscillator strengths $\tilde{f}$ (with $\tilde{f} > 0.01$) for the C_{2v} structure of Li_6, computed with "DFT-multiplets" and MRD-CI (from Ref. [1]). The corresponding transition energies (eV) obtained with DFT-"multiplets" and MRD-CI are also reported. All states are labelled within the C_{2v} group

DFT transition energy	DFT symmetry state	DFT oscillator strength	Normalized DFT oscl. strength	Summation due to degeneracy	MRD-CI transition energy	MRD-CI symmetry state	MRD-CI oscillator strength	Normalized MRD-CI oscil. strength	Summation due to degeneracy
1.52	A_1	0.515	0.096	0.096	1.42	$2A_1$	0.100	0.037	0.037
1.53	B_2	0.693	0.129	0.129	1.65	$1B_2$	0.046	0.017	0.017
1.73	B_2	0.167	0.031		1.73	$2B_2$	0.159	0.059	
1.77	B_2	0.569	0.106	0.137	1.79	$3B_2$	0.200	0.074	0.133
					1.80	$2B_1$	0.022	0.008	
					1.84	$4A_1$	0.031	0.011	
					2.11	$5A_1$	0.033	0.012	
					2.20	$6A_1$	0.031	0.011	
2.27	A_1	0.588	0.109		2.37	$7A_1$	0.076	0.028	
2.27	B_2	0.677	0.126	0.235	2.40	$5B_2$	0.600	0.221	0.249
2.36	B_1	0.527	0.098		2.43	$5B_1$	0.029	0.011	
2.41	A_1	0.609	0.113		2.51	$8A_1$	0.875	0.323	
2.50	B_1	0.631	0.117		2.59	$9A_1$	0.233	0.086	
2.50	B_1	0.407	0.076	0.404	2.62	$7B_2$	0.239	0.088	0.508
					2.93	$8B_1$	0.038	0.014	

Table 6. Comparison of normalized oscillator strengths $\tilde{f}$ (with $\tilde{f} > 0.006$) for the planar D_{3h} structure of Li_6, computed with DFT-"multiplets" and MRD-CI (from Ref. [2]). The corresponding transition energies (eV) obtained with DFT-"multiplets" or DFT-Fritsche (identified by (*)) and MRD-CI are also reported (see text). The MRD-CI states are labelled within the C_{2v} subgroup. The DFT states are labelled within the C_{3v} subgroup

DFT transition energy	DFT symmetry state	DFT oscillator strength	Normalized DFT-oscil. strength	Summation due to degeneracy	MRD-CI transition energy	MRD-CI symmetry state	MRD-CI oscillator strength	Normalized MRD-CI oscil. strength	Summation due to degeneracy
1.55	E	0.67	0.116	0.116	1.54	$1B_2$	0.11	0.036	
					1.59	$2A_1$	0.17	0.055	0.091
1.73	A_2	0.056	0.010						
1.90 (*)	E	1.795	0.311		2.15	$3B_2$	0.91	0.295	
2.13	A_1	1.173	0.203	0.514	2.19	$4A_1$	0.92	0.297	0.592
2.25	E	0.068	0.012	0.012	2.26	$4B_2$	0.03	0.010	
					2.36	$6A_1$	0.02	0.007	0.017
2.48	E	0.290	0.050	0.050	2.44	$7A_1$	0.02	0.006	
					2.46	$6B_2$	0.05	0.016	
					2.50	$2B_1$	0.06	0.020	
					2.54	$7B_2$	0.03	0.010	0.052
2.68	E	0.049	0.008	0.008	2.61	$8A_1$	0.02	0.008	0.008
2.80	E	0.290	0.050		2.81	$4B_1$	0.05	0.015	
2.80	E	0.264	0.046		2.88	$10A_1$	0.07	0.022	
2.86	E	0.295	0.051	0.147	3.08	$10B_2$	0.24	0.078	
2.96	A_1	0.818	0.142	0.142	3.04	$11A_1$	0.20	0.065	0.115
					3.15	$5B_1$	0.16	0052	0.117

conclusion does not hold for small intensity transitions, as can be seen in Table 3: rms deviation between the Fritsche and MRD-CI values: 34%, between the Fritsche and multiplet values: 33%.

4.2 Intensities

The "DFT-multiplets" normalized oscillator strengths for $Li_4(D_{2h})$, $Li_6(C_{2v})$ and $Li_6(C_{3v})$ are gathered in Tables 4–6 with those of Ref. [1, 2]. Most of them compare well with the high-level CI calculations. Only the two lowest energy transitions in $Li_6(C_{2v})$ are in total disagreement: $f_n = 0.096$ and 0.129 in our calculation compared to 0.037 and 0.017 (this point is still the subject of further study). These values excepted, the rms deviation is about 16% with a maximum equal to 29%: 0.012 (this work) and 0.017 (MRD-CI) for a weak transition in $Li_6(C_{3v})$. Obviously, the MRD-CI transitions involving mainly a doubly excited configuration have no equivalent components in this work, which considers only the one-electron excitations. On the other hand, "DFT-Fritsche" oscillator strengths are in reasonable agreement with MRD-CI results only for transitions corresponding to largest MRD-CI oscillator strengths, as illustrated in Table 7: the rms deviation between Fritsche and MRD-CI is about 20%. More precisely, since no splitting into states is performed with the Fritsche scheme, only the sum of the DFT transitions lying within a narrow interval has to be compared to the sum of the corresponding states involved in the MRD-CI approach.

4.3 Comparison of spectra

The computed absorption spectra in the visible range, obtained by convolution with a gaussian, are given in Figs. 1–4. For each cluster ($Li_3(C_{2v})$, $Li_4(D_{2h})$,

Table 7. Comparison of normalized oscillator strengths obtained with Fritsche approach and MRD-CI values (Ref. [1, 2]). This table has been limited to energy ranges corresponding to "MRD-CI summation oscillator strength" great in the range of 1

| Cluster	DFT-Fritsche transition energy range	DFT-Fritsche summation of normalized oscillator strengths	MRD-CI transition energy range	MRD-CI summation of oscillator strengths	MRD-CI summation of normalized oscillator strengths
Li_4 (D_{2h})	1.9	0.342	1.78	0.7926	0.370
Li_4 (D_{2h})	3.3–3.5	0.319	3.01	0.5698	0.266
Li_6 (C_{2v})	2.3–2.6	0.607	2.37–2.62	2.052	0.757
Li_6 (C_{3v})	1.9–2.1	0.602	2.15–2.19	1.83	0.592
Li_6 (C_{3v})	3.2–3.4	0.273	3.08–3.15	0.6	0.195
Li_8 (T_d)	2.2–2.5	0.780	2.41–2.63	3.801	0.738
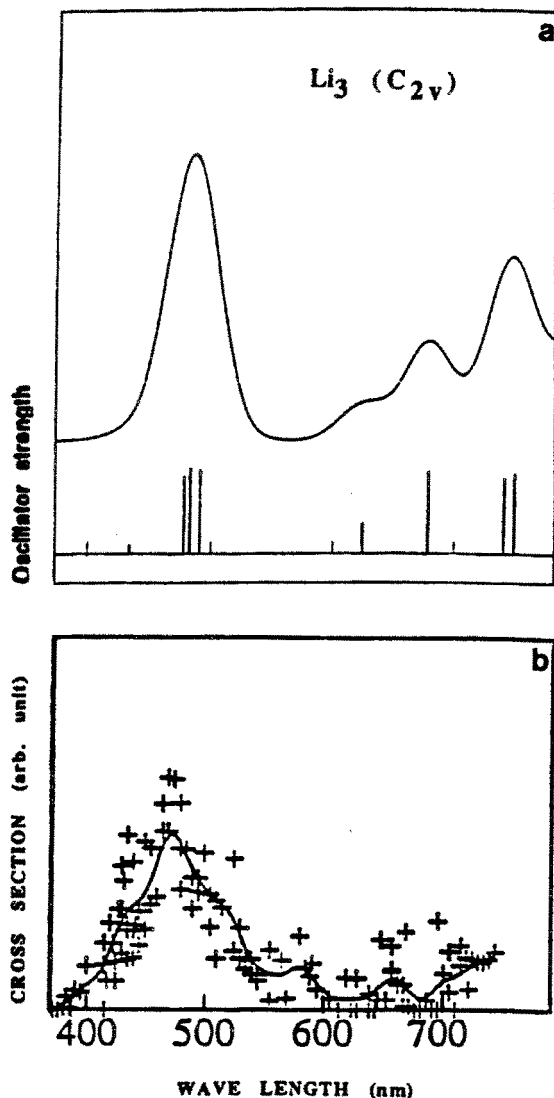
Fig. 1a, b. Comparison between: (a) DFT computed spectrum with "multiplets" approach for the more stable geometry of Li_3; (b) experimental spectrum from Ref. [4]

$Li_6(C_{2v})$, $Li_8(T_d)$), they proceed from our most stable geometries, very close to those of Ref. [1, 3], which have been proved to be the experimental ones. Two of the spectra have been obtained through the "multiplet" approach, which can be regarded as the best one (at least the more exact) due to its theoretical background, the two others within the approach of Fritsche. Analysis of spectra has been performed making use of the symmetry of transitions for comparison to CI results. Despite the following remarks, a reasonable agreement with the experimental data is found, as observed in Figs. 1–4:

– The $Li_3(C_{2v})$ spectrum (Fig. 1) describes well the experimental one of Ref. [4] but it should be noticed that the spectrum in Ref. [1] exhibits peaks lying at the same energy with different relative intensities.
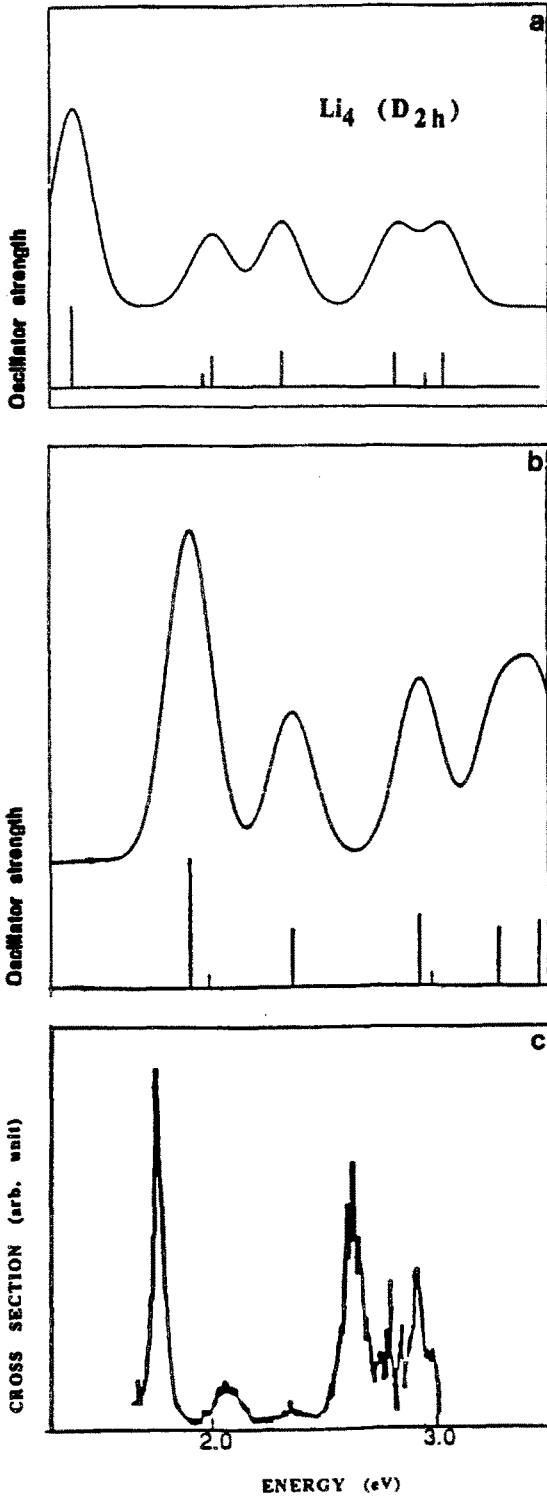
Fig. 2a–c. Comparison between: (a) DFT computed spectrum with "multiplets" approach for the more stable geometry of Li_4. (b) DFT computed spectrum with Fritsche approach; (c) experimental spectrum from Ref. [3]
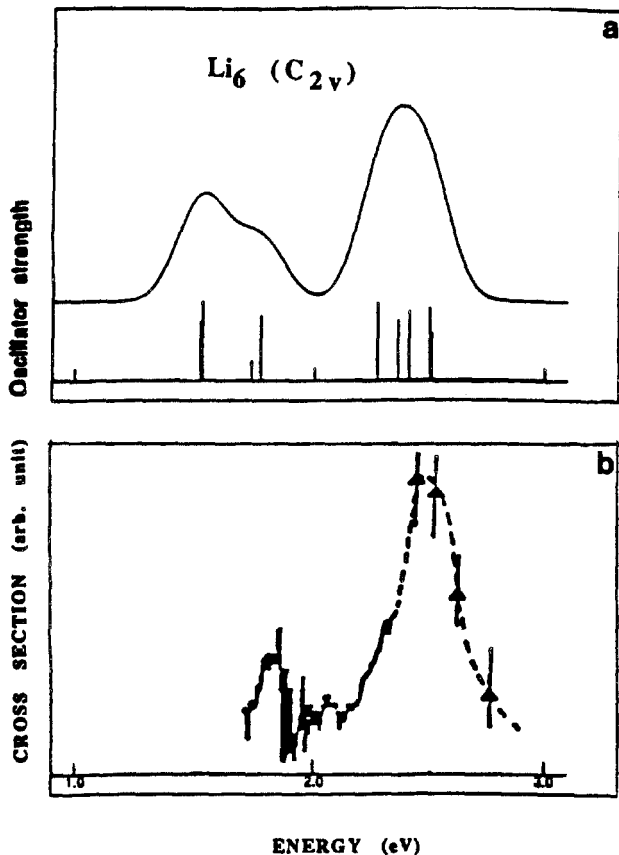
Fig. 3a, b. Comparison between: (a) DFT computed spectrum with "multiplets" approach for the stable geometry of Li_6; (b) experimental spectrum from Ref. [2]

– In $Li_4(D_{2h})$, as already said, some multiplets lie at too low energy (therefore leading to too small oscillator strengths) and only the peaks near 2.8–2.9 eV are correctly reproduced (Fig. 2a). The Fritsche approach (Fig. 2b) allows a coarse assignment of the main experimental transitions, but cannot reproduce the fine structure, at least because the four main peaks are shifted towards high energies.
– Figure 3 shows the $Li_6(C_{2v})$ spectrum in accord with the experimental one. However, the oscillator strengths at low energy disagree with the CI values. Unfortunately, this energy range has not been investigated experimentally in Ref. [2].
– In Fig. 4 is drawn the theoretical absorption spectrum of $Li_8(T_d)$. For this cluster, the Fritsche approach gives, for a moderate computational effort (with respect to the multiplet calculation and of course the CI one), a reasonable description of the broad-band spectrum. In T_d symmetry, a multiplet calculation should improve the accuracy of the spectrum, but because of the threefold degeneracy of some irreps, the calculation is more complicated than for cases like C_{2v}, and such a work is still in progress.
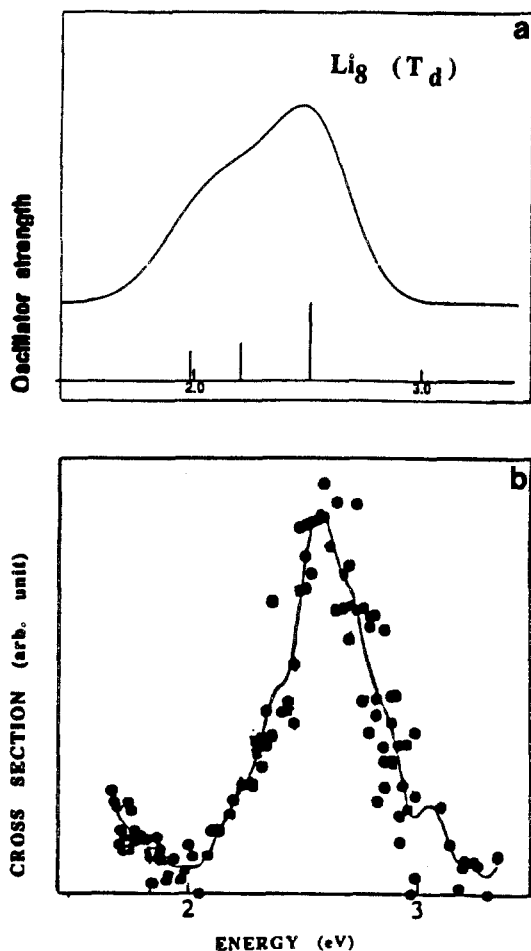
Fig. 4a, b. Comparison between: (a) DFT computed spectrum with Fritsche approach for the more stable geometry of Li_8; (b) experimental spectrum from Ref. [4]

5 Conclusion

The predictive power of DFT to give structural and spectroscopic assignments and interpret absorption spectra has been investigated through the example of small lithium clusters, within two different approaches, one of them bearing on the determination of the multiplet structure. Kohn–Sham orbitals are used to build wave functions of the ground state and excited states to compute the oscillator strengths of electric dipole transitions. It is shown that they are not directly comparable with MRD-CI results: only relative oscillator strengths can be compared in terms of "normalized oscillator strengths" in a narrow energy band. Then, DFT values with the multiplet method and in a smaller extent the Fritsche method are generally in reasonable agreement with MRD-CI results and experimental data.

On the other hand, from the comparison of transition energies given by the two DFT approaches and MRD-CI or experimental values, the following conclusions can be drawn:

(i) the multiplet method is capable of reproducing realistic energies and therefore, associated with oscillator strength calculations, it represents a suitable tool for the

prediction of absorption spectra. However, in a few cases ($Li_4(D_{2h})$ and $Li_6(C_{3v})$), a transition energy with a large oscillator strength may be found to be unsatisfactory, leading to a poor description of a part of the spectra. The neglect of the second-order electrostatic contributions to the multiplet energies or a weakness in the description of the correlation may explain such features.

(ii) The Fritsche scheme yields correct results only for the largest oscillator strengths and then leads to only a qualitative description of the absorption spectra. Nevertheless, energetic results show that formula (3), which has been demonstrated for solids and ignores the multiplet splitting, can give interesting preliminary information with a minimum computational effort, for a cluster.

(iii) Finally, this work shows that wave functions constructed from a set of Kohn–Sham orbitals can be reliable quantities for calculations of electronic properties, such as oscillator strengths.

References

1. Blanc J, Bonačić-Koutecký V, Broyer M, Chevaleyre J, Dugourd Ph, Koutecký J, Scheuck C, Wolf JP, Wöste L (1992) J Chem Phys 96:1793
2. Dugourd Ph, Blanc J, Bonačić-Koutecký V, Broyer M, Chevaleyre J, Koutecký J, Pittner J, Wolf JP, Wöste L (1991) Phys Rev Lett 67:2638
3. Dugourd Ph (1991) Thesis, University of Lyon
4. Vezin-Pintar B (1994) Thesis, University of Lyon
5. Ziegler T (1991) Chem Rev 91:651
6. Zhao Q, Parr RG (1992) Phys Rev A46:2337; Zhao Q, Parr RG (1993) J Chem Phys 98:543
7. Hohenberg P, Kohn W (1964) Phys Rev B 136:864
8. Baerends EJ, Ellis DE, Ros P (1973) Chem Phys 2:41; te Velde G and Baerends EJ (1992) J Comput Phys 99:84; ADF release 1.02; Department of Theoretical Chemistry; Vrije Universiteit; Amsterdam
9. St-Amant A, Salahub DR (1990) Chem Phys Lett 169:387; St Amant A (1991) Thesis; University of Montrial
10. Gunnarsson O, Lundqvist BI (1976) Phys Rev B13:4274
11. Ziegler T, Rauck A, Baerends EJ (1977) Theor Chim Acta 43:261
12. Von Barth U (1979) Phys Rev A20:1693
13. Daul C (1994) Int J Quant Chem 52:867
14. Daul C, Gudel HU, Weber J (1993) J Chem Phys 98:4023
15. Fritsche L (1991) Physica B172:7
16. Perdew JP (1991) In: Ziesche P, Eschig HH (eds) Electronic structure of solids, Akademic Verlag; Berlin
17. Becke AD (1988) Phys Rev A38:3098
18. Gardet G, Rogemond F, Chermette H, to be published
19. Nicolaides CA, Beck DR, Sinanoğlu O (1973) J Phys B Atom Molec Phys 6:62
20. Griffith JS (1964) the theory of transition metal ions, Cambridge University Press, Cambridge
21. Crossley R (1984) Physica Scripta T8:117
22. Bauschlicher Jr CW, Langhoff SR (1991) Theor Chim Acta 79:93
23. Fuchs C, Bonačić-KouteckýV, Koutecký J (1993) J Chem Phys 98:3121
24. Gerber WM, Schumacher E (1978) J Chem Phys 69:1692
25. Wolf JP, Delacritaz G, Wöste L (1989) Phys Rev Lett 63:1946
26. Malkin VG, Malkina OL, Casida ME, Salahub DR (1994) J Am Chem Soc 116:5898